Nuclear Mathematical and Computational Sciences: A Century in Review, A Century Anew
Gatlinburg, Tennessee, April 6-11, 2003, on CD-ROM, American Nuclear Society, LaGrange Park, IL (2003)

REACTIVITY VOID COEFFICIENT IN MOX CORES USING THE APOLLO2 CODE. ANALYSIS OF THE MISTRAL3 EXPERIMENT

A. Santamarina, A. Courcelle, E. Genero, O. Litaize, M. Palacin
CEA – Cadarache DEN/DER/SPRC
13108 Saint Paul lez Durance, France
alain.santamarina@cea.fr

ABSTRACT

This paper presents the analysis results of reactivity void coefficient in a core loaded with 100% MOX fuel. In a first step, the validation of the APOLLO2.5 calculation scheme is carried out against a reference continuous-energy Monte Carlo TRIPOLI4 calculation. Then, the experimental validation of the APOLLO2.5 prediction is performed using the MISTRAL3 measured worth and power maps.
Three configurations have been investigated : 0%, 60% and 100% local void. Concerning the APOLLO2 lattice calculation, the 0% void configuration uses the 2D-UP1 model (interface current method with linear anisotropic angular fluxes). In partial void situation, the exact 2D Pij method is required to obtain accurate results. In 100% void situation, every Pij calculation method supplies satisfactory results (a Wigner-Seitz cylindrization can be used).
The experimental validation of the APOLLO2.5 code deals with local void reactivity effect for 40%, 60% and 100% void in the 7x7 central cells of a 100% MOX core. APOLLO2-XY calculation of the MISTRAL3 core estimates accurately the void reactivity worth. Furthermore, the APOLLO2 calculation predicts the fission rate radial map within the ±2% uncertainty margin. However, in the 100% void experiment, the power is under-estimated (-10%) in the 7x7 voided zone. The RZ calculation, which accounts for the actual 3D effects, confirms this C/E disagreement.

Key Words: Void Coefficient, MOX, APOLLO2, TRIPOLI4, MISTRAL Experiment

1. INTRODUCTION

The French CEA and the Japanese NUPEC Nuclear Corporation jointly decided to undertake a programme called 'MISTRAL' starting in 1996 and pursued up to 2000 [1]. Four cores were investigated. The third core of this experimental programme, e.g. the MISTRAL3 configuration, is devoted to the measurement of fundamental parameters of an over-moderated 100% MOX lattice (square pitch : 1.39 cm, H/HM=6.0, Volumetric Moderator Ratio=1.8) loaded with PWR-7%Pu fuel pins. In this experiment, the local void is investigated in the central part, 7x7 fuel cells, of the regular lattice MOX core. Three void levels were studied: 40%, 60%, 100%.
In order to analyse the experimental results, the APOLLO2 reference calculation scheme "*CEA-97*" was implemented [2]. The recent APOLLO2.5 version and its associated CEA93.V6 library were used [3] [4].
The first part of this paper describes the MISTRAL3 experiment. The second part is devoted to the validation process against the Monte Carlo code TRIPOLI4. The qualification against the MISTRAL experimental results is presented in the last section.

2. THE MISTRAL3 EXPERIMENT

The MISTRAL experiments were performed in the EOLE zero-power experimental reactor at CEA-Cadarache.
The MISTRAL3 100% MOX core is a regular lattice configuration, with a square lattice pitch of 1.39 cm, characterized by the following loading pattern:

- 1388 MOX fuel pins with a 7% Pu enrichment (from reprocessing of UOX 35Gwd/T, with the following original isotopic vector : 1.4%^{238}Pu-57.7%^{239}Pu-24.5%^{240}Pu-10.1%^{241}Pu-5.3%^{242}Pu-1.0%^{241}Am),
- 16 guide-tubes devoted to the location of the safety clusters rods (enriched B_4C),
- 1 guide-tube devoted to the pilot rod (natural B_4C),

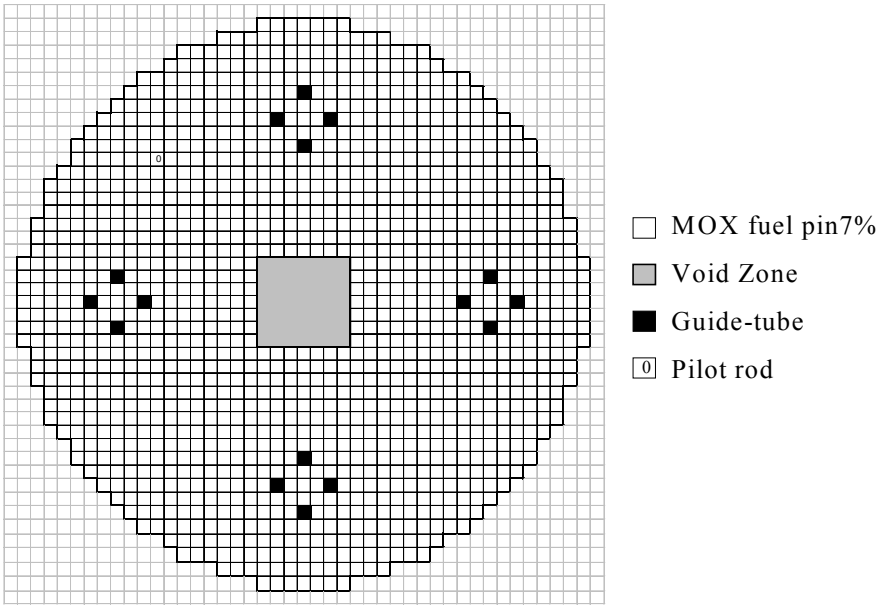

Figure 1. Radial cross section of the MISTRAL3 core

In order to insure that the temperature of the core remains constant during the experimental study, a thermoregulation system is implemented in the EOLE facility.
Five critical configurations were achieved : 2 reference cores (0% void) and 3 void patterns. These studies are specially devoted to the determination of the physical phenomena linked to the voidage of a central zone of 7x7 fuel pins up to 100% void. These void situations are obtained using specific devices : thick Al over-cladding of the MOX pins (40% and 60% void), and a watertight aluminum block where MOX pins are inserted for the 100% void configuration.

3. VALIDATION OF LATTICE CALCULATIONS

3.1. Theoretical Benchmarks

The TRIPOLI4 code [5], developed at the CEA, is a continuous energy Monte Carlo code. Stochastic resolution gives a reference solution of the problem but cannot ensure reasonable execution time. Thus, we have to use approximate deterministic methods allowing a faster resolution. The APOLLO2 code is a modular code which solves both the Boltzmann integral equation and the integro-differential equation. The modeling errors will be assessed by comparison with the reference continuous-energy Monte Carlo calculations.
The APOLLO2 code uses the CEA93.V6 library, which was processed from the JEF2.2 evaluations. We used the European X-MAS 172 group-structure. The TRIPOLI4 Monte Carlo continuous-energy calculation uses the same nuclear data file JEF2.2.
Three benchmarks have been carried out in order to validate the first step of the APOLLO2 calculation route, i.e the infinite lattice calculation :

- 0% void
- 60% void
- 100% void

The APOLLO2 reference calculation is defined by selecting the code options which yield known and acceptable errors (consistent with target accuracy). The APOLLO2 code allows the use of several collision probability methods to solve the integral equation. The most accurate one is the exact 2D Pij method in which the geometry described is the actual geometry of the lattice. In this method, no cylindrisation, nor isotropic interface angular flux assumption is used.
The comparison TRIPOLI4 / APOLLO2 is summarized on synthetic neutronic parameters. Reaction rates are condensed on a 13-group structure for the validation of the resonant absorption calculation.
The neutron balance breakdown is obtained through "six" factors (Fermi's four factor formula) :

$$K_\infty = \chi_{n,2n}\ \varepsilon_{fast}\ \varepsilon_{epi}\ p\ f\ \eta$$

The $\chi_{n,2n}$ factor is equal to the total absorption rate (neutron source S=1). The "ε_{fast}" fast fission factor takes into account U_{238}, Pu_{240}, Pu_{242} threshold fissions. The epithermal fission factor "ε_{epi}" takes into account U_{235}, Pu_{239}, Pu_{241} and Am_{241} fissions in the resonance range. The resonance escape probability is noted p. The thermal range below 0.625 eV is characterized by the neutron utilization factor f and the neutron reproduction factor η.

3.2. Result in the 0% Void Case

In this standard PWR lattice, the *CEA-97* reference route corresponds to an exact-2D Pij method and the space-dependent self-shielding calculation is also carried out in 2D geometry. The exact-2D Pij method is expensive in depletion calculation of LWR assemblies. Therefore, it is necessary to investigate the best multicell model within interface current assumptions : exact 2D calculations are needed inside each cell, and UP1 linear anisotropic interface fluxes are required. TRIPOLI4 results are obtained after the simulation of 3 millions of neutron histories. The calculation biases between APOLLO2.5 and TRIPOLI4 are reported in Table I (1 pcm = 10^{-5} in $\Delta K/K$).

Table I. Discrepancies between TRIPOLI4 and APOLLO2 calculations in LWR MOX lattice

	TRIPOLI4	Pij2D	Pij2D/T4 in pcm	UP1	UP1/T4 in pcm
X(n,2n)	1.001251	1.00110	-15	1.00112	-13
ε_{even}	1.064026	1.06364	-36	1.06414	10
ε_{uneven}	1.250650	1.25255	152	1.25248	147
p	0.570888	0.57021	-118	0.57007	-142
f	0.943275	0.94319	-9	0.94349	23
η	1.688429	1.68873	18	1.68875	19
K_∞	**1.211442**	**1.21133**	**-8**	**1.21197**	**44**

Table I shows that the same slight compensation of errors (about 100 pcm) between ε_{epi} factor and p escape factor arises in exact-2D and UP1. The overestimation of ε_{epi} factor is mainly due to a rough mutual shielding modeling : the Pu_{241} fission rate is overestimated by 10.4% in the macrogroup 13.7eV < E < 25.0eV, which leads to a 0.6% overestimation of the Pu_{241} total fission (due to the strong overlapping of the Pu_{241} and the Pu_{239} resonances at E_R=14.7eV). The underestimation of the escape factor p is also due to resonance overlapping : the Pu_{240} total capture rate is overestimated by 0.3% due to the strong overlap of the E_R=20.45eV and 66.2eV resonances with the E_R=20.9eV and 66.0eV resonances of U_{238}.

3.3. Results in the 60% void Case

The decrease of moderator amount induces a neutron spectrum hardening. Consequently, self-shielding of the unresolved resonances is required. The Monte Carlo code TRIPOLI4 can handle this phenomena through probability tables: Table II shows a K_∞ increase by 120 pcm ± 60 pcm.

Table II. Reactivity effect of TRIPOLI4 probability tables in the unresolved resonance range

K_∞ without probability tables	σ (pcm)	K_∞ with probability tables	σ (pcm)
1.02951	41	1.03075	49

Table III. Discrepancies between APOLLO2 and TRIPOLI4 calculations for the 60% void case

	TRIPOLI4	Pij2D/T4 (pcm)
X(n,2n)	1.00096	29
ε_{fast}	1.11524	17
ε_{epi}	1.75297	451
p	0.32353	-795
f	0.97055	11
η	1.67754	38
K_∞	**1.03075**	**-250**

The ε_{epi} factor (fissile nuclei) is overestimated in APOLLO2 by 450 pcm, owing to enhanced resonance overlapping effect in this intermediate spectrum.
The discrepancy on the resonance escape factor p amounts to –800 pcm. This bias is also due to the mutual shielding formalism : the Pu_{240} capture rate is strongly overestimated in the 20.5eV and 66.2eV resonances, respectively +22% and +17%. On the contrary, the U_{238} resonant capture is accurately predicted by the APOLLO2 powerful self-shielding formalism (AP2/T4 = +0.05% ± 0.07%).
One part of the escape factor disagreement is due to the Al_{27} capture rate : Table IV points out a large overestimation of the APOLLO2 capture in the macrogroup 3 (5 keV < E < 0.9 MeV), which induces –100 pcm bias on the escape factor in this lattice with a large amount of Al (thick Al over-clad).

Table IV. Discrepancies between APOLLO2 and TRIPOLI4 on Al_{27} absorption rate

Group n°	TRIPOLI4 Absorption rate	TRIPOLI4 1σ in %	Pij2D / T4 Bias in %
1	9.61485E-05	1.59	-0.7
2	1.50963E-03	0.22	0.2
3	1.28264E-03	0.18	8.2
4	1.36887E-04	0.06	-0.2
5	2.00013E-04	0.07	-0.5
⋮	⋮	⋮	⋮
Sum	9.10321E-03	0.07	11.6

In this under-moderated lattice, similar to HCPWR lattice, an accurate spatial modeling is required in resonance absorption calculation due to enhanced Dancoff effect; Table V shows the APOLLO2 results using various Pij approximations : interface current patterns (UP0 and UP1) and standard cylindrical pin-cell model (CYL) are compared to exact-2D Pij.

Table V. Discrepancies (in pcm) betweenTRIPOLI4 and various APOLLO2 Pij models (60% void case)

	TRIPOLI4	**CYL/T4**	**UP0/T4**	**UP1/T4**	**Pij2D/T4**
X(n,2n)	1.00096	30	30	30	29
ε_{fast}	1.11524	176	142	98	17
ε_{epi}	1.75297	2378	1713	942	451
p	0.32353	-4511	-3407	-1825	-795
f	0.97055	301	217	84	11
η	1.67754	-110	-58	-1	38
K_∞	**1.03075**	**-1852**	**-1426**	**-690**	**-250**

Table V indicates that exact 2D Pij calculation is required in partial void situations. Multicell method raises large discrepancies in resonance absorption, even in the linear anisotropic interface flux model (mainly due to the assumption of uniform current on each cell side). The

implementation of a cosine incoming current assumption (UP0 and CYL) is not suited for calculation of under-moderated lattices : the escape factor p is underestimated by 3400 pcm; 1D-Pij calculation inside cells increases the p bias up to –4500 pcm.

3.4. Result in the 100% void Case

In the benchmark, the void is simulated by aluminium. The neutron spectrum could be considerer as a fast reactor spectrum. Therefore, the neutron multiplicity increases and the (n,γ) capture decreases. Consequently, nuclei reproduction factor η_i increases quickly. Due to competition between U_{238} and Pu_{239} absorption, the void coefficient will remain negative for Pu enrichment below 13%.
TRIPOLI4 reference results (using probability tables in unresolved range) are compared to APOLLO2 results using various Pij models in Tables VI, VII.

Table VI. K_∞ comparison between APOLLO2 and TRIPOLI4 (100% void case)

K_∞ TRIPOLI4	σ (pcm)	Pij2D/T4	UP1/T4	UP0/T4	CYL/T4
0.68374	38	-97	-5	-35	-41

Table VII. Discrepancies between APOLLO2 and TRIPOLI4 calculations (f : capture in Al and Zr)

	TRIPOLI4	CYL/T4	UP0/T4	UP1/T4	Pij2D/T4
X(n,2n)	1.00140	-3	-3	-3	-3
ε	1.31859	349	349	366	347
p	0.28065	901	903	918	862
f	0.95138	-1146	-1140	-1145	-1172
η	1.93931	-130	-131	-129	-119
K_∞	**0.68372**	**-41**	**-35**	**-5**	**-97**

Whichever Pij model is used, there is no significant discrepancies amongst APOLLO2 results. Even a Wigner cylindrical model can be used in this 100% void situation.
Table VII shows that the f factor is strongly underestimated by APOLLO2, about 1170 pcm. This problem is linked to the Al_{27} treatment in multigroup codes : the total capture in Al block amounts to 1601 pcm and 2858 pcm respectively in TRIPOLI4 and APOLLO2. Furthermore, a significant disagreement is raised on ε (threshold fissions) and p factor (fertile absorption / actinide absorption), due to Al slowing-down contribution in the APOLLO2 multigroup calculation which is biased by unshielded scattering cross sections.
Therefore, the implementation of Al self-shielded cross sections is required in deterministic codes, even in the XMAS 172-group structure.
In order to check this conclusion, we replaced the Al_{27} block by air, as shown in Table VIII.

Table VIII. Comparison between TRIPOLI4 and APOLLO2 Pij in fast spectrum (100% void case)

	TRIPOLI4	CYL/T4	UP0/T4	UP1/T4	Pij2D/T4
X(n,2n)	1.00192	73	73	73	73
ε	1.45313	150	150	151	156
p	0.27938	420	419	420	369
f	0.96655	-38	-37	-38	-60
η	2.10052	-260	-260	-260	-246
K_∞	**0.82582**	**345**	**345**	**345**	**291**

The discrepancies between APOLLO2 and TRIPOLI4 concerning ε, f and η are now satisfactory, respectively +156 pcm, –60 pcm and –246 pcm.
However, there is still a slight disagreement by +370 pcm on the escape factor p, which is due to APOLLO2 lower U_{238} capture rate (-0.72% ± 0.04%) in the 100 keV-5 keV unresolved resonance range.

4. EXPERIMENTAL VALIDATION ON MISTRAL PROGRAMME

The outstanding capabilities of the APOLLO2 code allow us to perform the whole MISTRAL3 experiment analysis in transport theory, including the basic fuel lattice and multicell calculations (guide tubes and reflector region), as well as the whole core calculation.

In the Pij lattice calculation phase, a procedure is used to take into account automatically the variation of boron (including the reflector), the ageing of MOX fuel, the variation of the water density and the effects of thermal expansion.
The core calculation is carried out using S_N method in the reference *CEA-97* scheme :

- S8 quadrature for the angular approximation
- P1 anisotropic scattering
- Nodal method (instead of diamond finite difference) allowing 1 mesh point per cell
- 20 energy groups for the multigroup approximation.

4.1. Analysis of void worth measurements

In the framework of the MISTRAL3 experiment, five critical configurations were achieved by adjusting the boron concentration : 0%void (reference), 40%, 60%, 100%, then 0%. The void reactivity worth is obtained from the equivalence with soluble boron poisoning.

For each XY geometry core calculations, the variation of the axial buckling B^2_z in voided configurations due to the reduction of the axial reflector boron concentration is accounted for :

$$\Delta B_Z^2 = 0.0085\ 10^{-5}\ cm^{-2} / \text{ppm of boron} \quad \Rightarrow \quad \frac{\Delta K_{eff}}{K_{eff}} \cong \frac{-M^2 \Delta B_Z^2}{1+M^2 B^2} = -0.275 pcm / ppm$$

Since the experimental mean boron efficiency is $d\rho/dC_B$ = -8.3 pcm/ppm , this reflector saving effect corresponds to 3% of the void reactivity worth.

The Calculation-Experiment comparison of the core residual reactivity for the Reference configuration and the Voided configuration yields the absolute error C-E on void worth. The relative error is deduced as : $(C-E)/E = (C-E)/\rho^{Void}$

The magnitude of the void reactivity worth is obtained from the variation of the critical boron concentration : $\rho^{Void} \cong \Delta C_B \times \left(\frac{d\rho}{dC_B}\right) + \Delta\rho^{residual}$

with : - $\Delta C_B = C_B(REF) - C_B(Void)$: variation of the boron concentration

- $d\rho/dC_B$: mean boron efficiency (experimentally evaluated)
- $\Delta\rho^{residual} = \rho^{residual}(void) - \rho^{residual}(REF)$

The Calculation–Experiment comparison of the worth measurements is summarized in Table IX. The quoted uncertainties corresponds to measurement uncertainties, mainly soluble boron concentration and core residual reactivity, and do not account for technological uncertainties (external diameter of Al overclad,…).

Table IX. Reactivity void coefficient analysis with APOLLO2 code

APOLLO2 Reference scheme 'CEA-97' : Pij-UP1, S8P1-XY		
Configuration	$\rho_{void,exp}$	(C-E)/E
40% void	- 660 pcm	+7.5% ± 1.4% (1σ)
60% void	-1050 pcm	+2.8% ± 0.8% (1σ)
100% void	-1410 pcm	+1.3% ± 0.5% (1σ)

The analysis of the 40% void experiment shows that the APOLLO2 calculation over-estimates the partial void reactivity effect by 7%.
Concerning the 60% void experiment, the APOLLO2 over-estimation of the void worth decreases to 3%. In this high-level partial void, the UP1 interface current calculation is not suited, as pointed out in the previous validation work against TRIPOLI4 reference calculation; therefore, the recommended exact-2D Pij lattice was used in the lattice calculation. The results of both calculation routes are compared to the experimental values in Table X. The over-estimation of the void worth is reduced to 1.9% instead of 2.8% using UP1 multicell model.

Table X. Reactivity void coefficient analysis in the 60% void experiment. Exact 2D Pij

Configuration	$\rho_{void,exp}$	Calculation scheme	(C-E)/E
60% void	-1050 pcm	Pij2D - S8P1	+1.9% ± 0.8% (1σ)
		UP1 - S8P1	+2.8% ± 0.8% (1σ)

For the 100% void configuration, the most penalizing case for safety concern, the calculation over-estimates very slightly the reactivity void effect (≈1%). In order to check 3D and streaming effects, a RZ core calculation was performed. The results presented in Table XI confirm the satisfactory result obtained in the XY model. Thus, the local void reactivity effect is accurately predicted by the APOLLO2.5/CEA93 product, using its reference calculation scheme *'CEA-97'*.

Table XI. 100% void coefficient analysis, using XY and RZ geometry calculation

Configuration	$\rho_{void,exp}$	Calculation scheme	(C-E)/E
100% void	-1410 pcm	UP1-S8P1, XY geom	+1.3% ± 0.5%(1σ)
		UP1-S8P1, RZ geom	+0.9% ± 0.5%(1σ)

4.2. Analysis of the radial fission map

The radial distribution of the fission rates is obtained by integral gamma-spectrometry measurements directly on the fuel rods at middle height of the core.
The XY APOLLO2 calculations reproduce the tendency of the experimental results, in particular the strong decrease of the fission rate in the 7x7 voided zone. However, C/E comparison points out a trend to increasing overestimation of the fission rate with high void level (Figure 2). In the voided zone, the decrease of the local power with the void fraction is due to the loss of moderator: the thermal neutron flux and ^{239}Pu thermal fissions decrease quickly. In the 100% void case, the neutron spectrum at the center of the voided zone is almost a fast spectrum.

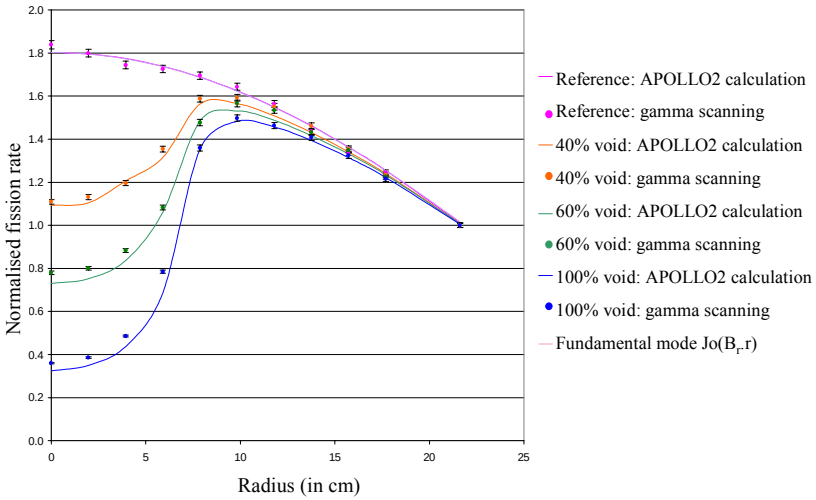

Figure 2. Radial distribution of fission rates in 0%, 40%, 60% and 100% void

In order to compare calculated and measured fission rates, these fission rates were normalized to the same value on 3 asymptotic fuel pins (noted * in the next figures), not disturbed by the proximity of the reflector and the voided zone.
The C/E comparison on radial power map in the 40% void configuration is shown in Figure 3. We notice that in the non disturbed zone, the APOLLO2 calculation reproduces correctly the distribution of fission rates (J_0 Bessel function). In the voided zone, we observe a 3% underestimation of the fission rate for MOX pins located at the "water/void" interface.

37												+0.8 *
36												
35										+0.4 *		
34									-1.0 *			
33								-2.1				
32							-2.7					
31						-1.7						
30					-1.6							
29				-2.9								
28			+0.8	-3.4		-0.2						
27		-2.3	-4.8	-3.4	-1.0	-0.5						
26	-1.5	+0.8	-2.8	-3.2	+0.5	-0.3						
	26	27	28	29	30	31	32	33	34	35	36	37

Figure 3. 40% void configuration. Calculation-Experiment comparison [(C-E)/E] in %

In the 60% void configuration, the fission rates are gradually under-estimated from the boundary to the centre of 7x7 the voided zone, from –3% up to –6% as shown in Figure 4.

37												+0.9 *
36												
35										+0.7 *		
34									-1.3 *			
33								-1.1				
32							-3.1					
31						-2.1	-3.7					
30					+0.5	-0.2	-0.7					
29				-2.0	+3.4	+0.4						
28			-5.2	-5.0	-0.4	-0.6	-1.0					
27		-6.0	-5.3	-2.4	+2.5	+0.7	-0.6					
26	-6.4	-6.2	-5.6	-3.6	+1.6	-1.0	-0.8	-0.8	-1.6			
	26	27	28	29	30	31	32	33	34	35	36	37

Figure 4. 60% void configuration. Calculation-Experiment comparison [(C-E)/E] in %

For the 100% void configuration (Figure 5), a clear trend to 4% power overestimation is now stressed on the first row of moderated cells. On the contrary, the fission rate is underestimated by 10% in the whole voided lattice. A validation study has pointed out that this C/E disagreement cannot be explained through energy collapsing (from 172g to 20g) or S8/P1 quadrature in the Sn core calculation. The discrepancy would be probably linked to standard cell homogenization.

37												+0.3 *
36												
35										+0.5 *		
34									-0.8 *			
33								-1.0				
32							-0.4					
31						-1.0	-0.3					
30					-0.4	-2.6	+0.2					
29				-12.5	+1.6	-0.1						
28			-9.9	-11.3	+3.0	-0.7	+0.2					
27		-9.3	-10.3	-11.5	+3.7	-0.3	-0.5					
26	-10.0	-9.7	-9.9	-11.7	+6.5	+1.0	-1.0	-0.5	-1.0			
	26	27	28	29	30	31	32	33	34	35	36	37

Figure 5. 100% void configuration. Calculation-Experiment comparison [(C-E)/E] in %

For this 100% void configuration, the RZ geometry calculation, more suited for 3D effects, has confirmed the underestimation in XY calculation of the power in the voided fuel lattice : at middle height of the core, the fission rate of the central pin is underestimated by -11% as shown in Figure 6.

37												+0.3 *
36												
35										+0.5 *		
34									-0.7 *			
33								-0.9				
32							+0.3					
31							-0.4					
30							+0.8					
29												
28							+0.5					
27							-0.8					
26	-11.1						-1.4	-0.5	-1.0			
	26	27	28	29	30	31	32	33	34	35	36	37

Figure 6. 100% void configuration. RZ calculation. [(C-E)/E] in %

4.3.Analysis of the axial fission rate distribution for the 100% void case

Measurements of the axial flux distribution aim at experimental investigation of 3D and streaming effects.

The axial distribution of fast flux was measured using miniature fission chamber with ^{237}Np deposit. This measurement, inside a guide tube replacing the fuel pin of the central voided cell, allows streaming effect analysis. The comparison of the APOLLO2 RZ results and of the ^{237}Np measurements shows that the calculation reproduces correctly measured axial fast flux. Figure 7 shows that flux profile deviates from the fundamental mode $Cos(B_z.z)$ (with $B_z^2 = 0.00107$ cm^{-2} in the moderated core), due to the moderator lack in the axial reflector.

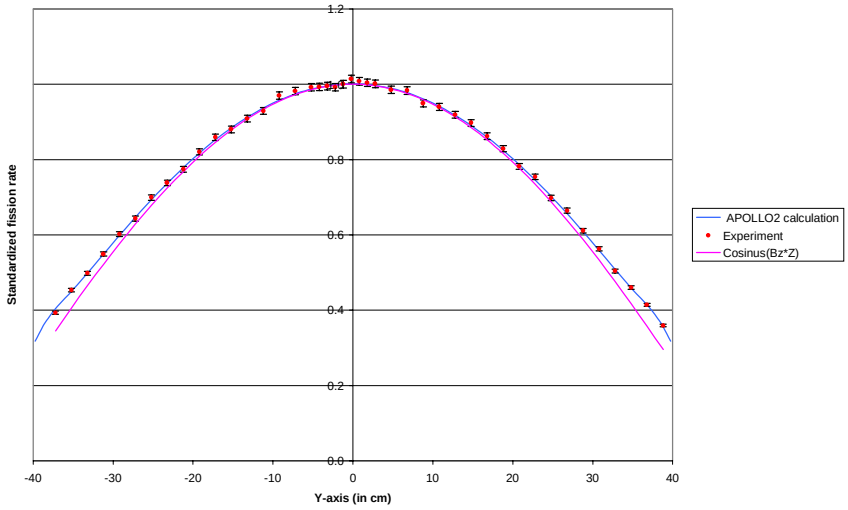

Figure 7. Axial distribution of the ^{237}Np fission chambers at the center of the voided zone

In order to investigate 3D effect, axial profile was measured for 4 fuel pins, from the central voided cell to the peripheral moderated lattice : axial fission rate distributions were obtained by integral gamma spectrometry on the fuel pins.

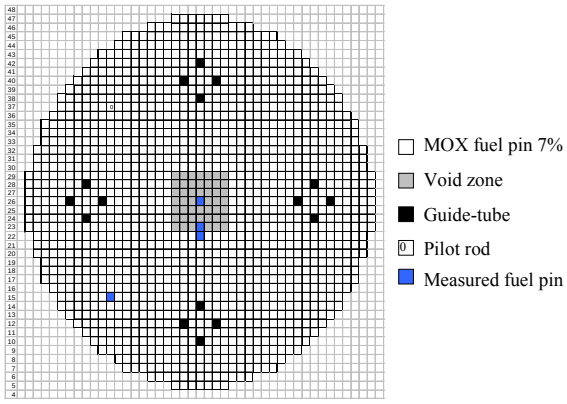

Figure 8. Location of fuel pins measured by axial gamma-spectrometry

The Calculation – Experiment comparison is plotted in Figure 9 (fission rates are normalized to unity at core middle height). The axial shapes versus core radius show that the flux is flattening when measurement location moves from asymptotic moderated fuel pin to the center of the voided zone. This 3D effect is well reproduced by the APOLLO2 calculation : this C/E agreement explains the satisfactory results obtained in the calculation of the reactivity void worth.

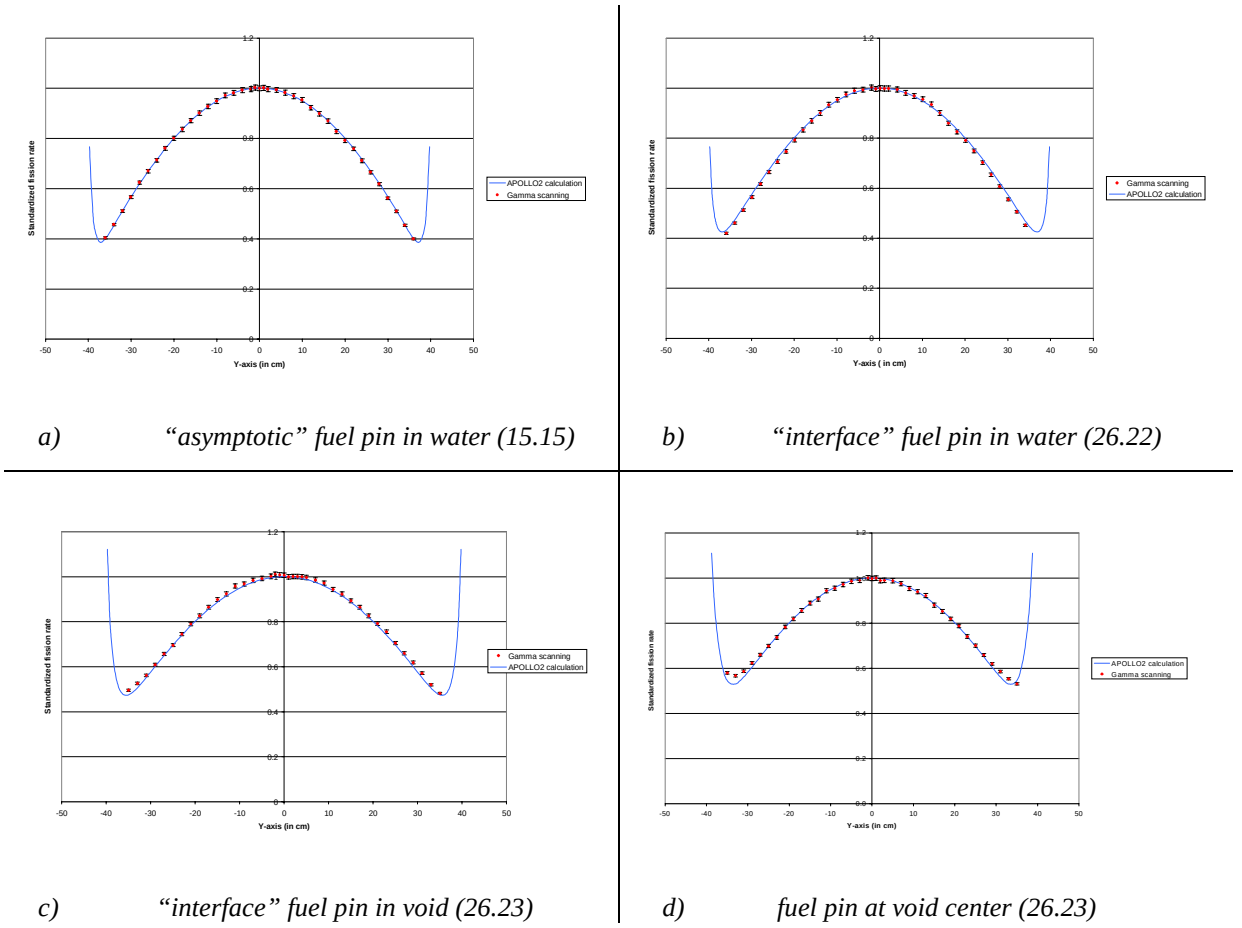

a) *"asymptotic" fuel pin in water (15.15)*

b) *"interface" fuel pin in water (26.22)*

c) *"interface" fuel pin in void (26.23)*

d) *fuel pin at void center (26.23)*

Figure 9. C/E comparison of axial power distribution in dry and moderated lattices

5. CONCLUSIONS

The validation study against the reference continuous-energy Monte Carlo code TRIPOLI4 has demonstrated that the UP1 interface current model is satisfactory in well-moderated LWR lattices. However, in partial void situations, only the exact-2D Pij model gives accurate results; the multicell models become inaccurate due to the uniform flux assumption on each cell side. In the 100% void situation, any Pij calculation method is adequate, even a Wigner cylindrization is sufficient.

The APOLLO2 multigroup treatment of Aluminum induces large biases : Al27 capture rate is overestimated in partial void situations, and its slowing-down important contribution in 100% void case is badly described.

These studies allowed the enlargement of the validation range of the APOLLO2.5/*CEA-97* package toward fast neutron spectra and FBR lattices.

Concerning the experimental validation of APOLLO2.5 and its CEA93.V6 library, the three experimental configurations, 40%, 60% and 100% void, in MISTRAL3 core were analyzed. The measurements dealt with reactivity void worth, radial fission rates and axial flux profiles.
The analysis of void worth enabled the qualification of the APOLLO2 calculation of LWR-MOX void coefficient for partial or total local void. The reactivity worth of large partial void, typically 60% void, is slightly overestimated by +3% ± 0.8%. In 100% void case, the C/E agreement lies within the 1% experimental uncertainty margin.
The measured axial and radial fission distributions are well predicted by the APOLLO2.5 calculation. However, in the 100% void configuration, the radial power map is under-estimated by 10% in the dry lattice ; fortunately, this C/E discrepancy does not impact significantly the void coefficient calculation. This disagreement in the low power level inside the voided lattice was not found in the MVP Monte Carlo analysis carried out by the Japanese team [6].

ACKNOWLEDGMENTS

The authors acknowledge the French industrial Partners CEA, EdF and Framatome for their financial support. The authors are indebted to the Eole experimental team, particularly Drs Blaise, Cathalau and Fougeras.

REFERENCES

1. S. Cathalau, J.C. Cabrillat, J.P. Chauvin, P.J. Finck, P. Fougeras, G. Flamembaum, H. Matsu-Ura, M. Ueji, T. Yamamoto, “MISTRAL : An Experimental Program in the EOLE Facility Devoted to MOX Core Physics,” *Proc. of Int. Conf. on the Physics of Reactors PHYSOR'96*, Mito (Japan), Sept. 16-20, pp. U-84 (1996).
2. O. Litaize, A. Santamarina, C. Chabert, “Analysis of the Mistral experiment with APOLLO2. Qualification of the neutronic parameters of UOX and MOX cores,” *Proc of ANS Reactor Physics Meeting PHYSOR2002*, Seoul (Korea), October 7-10 (2002).
3. R. Sanchez and al., “APOLLO-II: A User-Oriented, Portable, Modular Code for Multigroup Transport Assembly Calculations, ” *Proc. of Int. Top. Mtg. Advances in Reactor Physics, Mathematics and Computation*, Paris (France), April 27-30 (1987).
4. A. Santamarina, C. Chabert, A. Courcelle, O. Litaize, G. Willermoz, “Qualification of the APOLLO2.5/CEA93.V6 for UOX and MOX fuelled PWRs,” *Proc of ANS Reactor Physics Meeting PHYSOR2002*, Seoul (Korea), October 7-10 (2002).
5. J.P. Both, H. Derriennic, B. Morillon and J.C. Nimal, “A Survey of Tripoli4, ” *Proc. of Int. Conf. on Radiation Shielding 8*, Arlington (USA), Apr. 24-28, Vol. 1, pp. 373-380 (1994).
6. K. Hibi, M. Tatsumi, T. Umano, A. Fushimi, T. Yamamoto, M. Ueji and Y. Iwata, “Analysis of Mistral and Epicure Experiments with SRAC and MVP Code Systems,” *Proc. Int. Conf. Physics of Reactor Operation PHYSOR2000*, Pittsburg (USA), May 7-11, IX.E (2000).